EUROPEAN ORGANIZATION FOR NUCLEAR RESEARCH

CERN-PPE/93-139
July 5th, 1993

PERFORMANCE OF A LHC FRONT-END RUNNING AT 67MHz

The RD20 Collaboration

R. Brenner[1], J. Kaplon[2], H. von der Lippe[3], E. Nygård[4], S. Roe[1],
P.Weilhammer[1], K.Yoshioka[1]

ABSTRACT

The prototype version of a novel front-end system, designed for the readout of silicon microstrip detectors at the LHC, has been tested using 100 GeV pions incident on a microstrip detector in the X5 beam line at CERN. The prototype consisted of preamplifier and shaping amplifier with 45 nsec time constant, an 84 cell analogue pipeline and analogue pulse shape processor, with the individual elements of the system implemented as separate electronics chips. The timing conditions in the test were set up to simulate those in hadron collider experiments and a clock speed of 67 MHz was used. Deconvolution of particle signals from a silicon detector was successfully demonstrated for the first time in LHC-like experimental conditions.

Submitted to Nuclear Instruments and Methods A

---

1) CERN, Geneva, Switzerland
2) Institute of Nuclear Physics, Cracow, Poland
3) Senter for Industriforskning, Oslo, Norway. Now at Lawrence Berkeley Laboratory, Berkeley CA, USA
4) Senter for Industriforskning, Oslo, Norway. Now at Oslo University, Oslo, Norway

1. INTRODUCTION

The RD20 collaboration has proposed a novel front-end electronic architecture for reading out silicon detectors in a LHC experiment. A low power consumption with good signal to noise ratio will be obtained with a slow shaping preamplifier. The time resolution needed will later be extracted by deconvolution of the slow pulse. A prototype front-end chain in separate elements was tested in a 100 GeV pion beam at the X5 beam line at CERN. The purpose of this beam test was principally to demonstrate the operation for the first time of this signal processing scheme under semi-realistic conditions but some studies of pulse height observations in the test were also possible. The data obtained in the testbeam were also used later as a reference for minimum ionizing particles for tests in laboratory environment.

The elements of the electronic system were a preamplifier and shaping amplifier [1], an Analogue Delay and Buffer (ADB) [2] and an Analogue Pulse Shape Processor (APSP) [3]. The electronics was connected to a p^+-implanted AC-coupled detector [4] which had been irradiated with electrons to a dose of 50 kGy (5 Mrad). The strip length was 4 cm and the strip pitch 50 μm. The width of the p^+-implant was 10 μm. The prototype front-end chips were four channels wide but data was stored from only two of them because of the limited number of ADC channels available.

2. THE RD20 FRONT-END ARCHITECTURE

The principle of the RD20 front-end system can be found elsewhere [3]. The basic concept is to obtain low noise at low power consumption by using a 45 nsec CR-RC shaping of the preamplifier pulse. With the assumption that the time between beam crossings at the LHC will be 15 nsec, the 45 nsec shaped pulse does not unequivocally identify the interval in which a track measured in a detector originated. The time and charge information of the signal have therefore to be recovered by a deconvolution algorithm implemented as purpose-built integrated circuit, the APSP. The shaped pulse cannot be continuously deconvoluted because the very high speed needed would consume excessive power. The preamplifier signal is instead delayed by 1-3 μsec, which is the estimated time between first level triggers at LHC, in a pipeline buffer, the ADB, before entering the APSP. In the present prototype version of the pipeline a 1 μsec delay is implemented. The length of the delay is the estimated time for obtaining the first level trigger decision, T1, in a LHC experiment. If the first level trigger comes, four delayed samples associated with the event indicated by first level trigger are marked and later transferred to the APSP. If there is no trigger the samples are overwritten after 1 μs. The amount of data reaching the APSP is now reduced by a factor of about 1000 assuming an average trigger rate of 100 kHz. A schematic of the circuit is shown in Figure 1.

3. TESTBEAM

3.1 The Set-Up

Pulse generators and hodoscopes were used to emulate the LHC timing conditions in which the proposed tracking system could be embedded. The set-up was divided into two parts shown in Figures 2 and 3. One part, placed at the beam, consisted of a detector connected to the preamplifiershaper, scintillators and electronics to form coincidences between discriminated signals from the preamplifier-shaper and hodoscopes. The second part, placed outside the beam area, consisted of the ADB- and APSP circuits with pulse generators for external clocking and digital oscilloscopes connected via GPIB interfaces to a personal computer.

The set-up was run with a pulsed BCO clock generator instead of a continuous running BCO clock. The second option would have been preferable but in the short time available for this beam test the pulsed BCO clock was easier to tune to the right timing. By using the pulsed BCO clock the data collected was always stored in the same cells in the ADB. On the other hand it has been shown [5] that the effect of variations between the storage cells in ADB is much less than 1mV r.m.s., which is negligible compared to the noise from the front-end amplifier.

A Start-T1 signal was recorded in any of the readout channels of the detector in coincidence with both scintillators. Because of the delay in starting the pulse generators the start-BCO-signal had to be given as early as possible. This was done using the signal from one of the scintillators before any delaying logic. The signal from the preamplifier-shaper was delayed by 400 ns with a thick BNC cable in order to have the rest of the chain ready for the data. When the BCO clock was started a RESET pulse was immediately generated to clear the circuits. The TRIGGER 1 pulse was delayed to match the analogue pulse arriving from the preamplifier-shaper. Finally the Read Clock was started transferring data from the ADB to the APSP. The Read Clock in this test was chosen to run at 1 MHz asynchronously with the BCO clock.

The pulse shapes were sampled at three nodes of the system and stored for off-line analysis; after the preamplifershaper, after the ADB and at the output of the APSP. The digitisation of oscilloscope readings the amplifier-shaper signal was clocked externally by the BCO clock and the signals coming from the ADB and the APSP were externally clocked by the read-out clock. The oscilloscopes were externally triggered by the Start-T1 signal.

3.2 Results

In the short duration of time of this testbeam about 3000 events were recorded. However, because of problems ensuring that the two digital oscilloscopes, using separate time bases, should trigger simultaneously for data acquisition, some of the data were lost. This had a small impact on the detailed analysis of the signal to noise in the system and did not prevent the demonstration of its functionality.

The histograms shown in Figure 1 show the averaged pulse shape of all the data recorded in the testbeam. The three cross-hatched bins in the amplifier-shaper data and in the ADB data are the bins transferred through the system to the APSP. The single-hatched bin is stored for accurate pulse height determination in low luminosity conditions when no pileup of events is likely. Figure 4 shows the pulse heights in two neighbouring channels of a typical single event observed at different parts of the system showing clearly the observation of an in-time event which was successfully deconvoluted. The event is shown as seen after the amplifier-shaper, ADB and the APSP. The pulse height after the APSP is higher than the pulse height of the pulse in the amplifier-shaper and the ADB. This is due to the gain in the APSP being about 10 times higher than the rest of the chain. The APSP is only giving the deconvolution for the 15 ns time bin tagged by the T1 trigger. No information on the contamination of the neighbouring bin can be extracted unless the T1 trigger is scanned across the pulse. The T1 scan is explained later in this paper.

The pulse height information from the system was studied off-line in more detail to make a more quantitative assessment of the performance of the electronic chain. Since no absolute timing was recorded in the test, some assumptions had to be made to select events with the correct timing with respect to the BCO. To achieve this the samples at the output of the ADB were used. The selection of useful events made use of the known signal pulse shape by requiring the third sample given to the APSP to be between 50% and 85% of the maximum recorded pulse height. By this assumption about 50% of the non corrupted data was used for the analysis. Because of a bad groundplane on the printed circuit board for the APSP the single channel data was spoiled by pick-up from the beam. The effect of the pick-up was correlated in the two readout channels. Some quantitative results could still be saved by subtracting the two APSP channels. In this case the total pulse height decreases because some charge information from the neighbouring strip is subtracted. Figure 5 shows the pulse height of the channel with the bigger pulse when the pulse height from one neighbouring strip is subtracted for the amplifier-shaper, the ADB and the APSP samples.

Finally the functionality of the APSP circuit in this testbeam can be demonstrated by comparing the calculated response from the APSP with the measured response. The pulse height of the APSP is calculated using the pulse height of the three samples given to the

APSP. In the calculations the same deconvolution algorithm implemented in the APSP circuit is used. The correlation plot is shown in figure 6.

4. LABORATORY TESTS

4.1 The Laboratory Set-Up

The set-up in the testbeam was tested with a ^{104}Ru β-source in the laboratory. In order to obtain straight tracks the source was collimated. Two scintillators were used in this set-up, one thin and one thick scintillator, in coincidence with the readout channels of the detector to generate a trigger. The noise for the preamplifier-shaper, the ADB and the APSP was measured without source trigged randomly. The set-up was unchanged from the testbeam although the set-up had been rebuilt in the laboratory and the gain settings of the ADB and the APSP were change due to different biasing. The electron irradiated detector from the testbeam and a new non irradiated detector were tested in the laboratory. The geometry of the two detectors were identical with total leakage current going to the backplane for the electron irradiated detector 1.2 μA and for the non irradiated detector 1.8 μA at 100 V.

4.2 Laboratory Results

The data obtained with source is comparable with the data from the testbeam, figure 7. More care had been put into setting up the timing of the system giving a narrower trigger window than in the testbeam. The data was analysed using the same cuts as the testbeam data, which with the improved timing condition resulted in 80% of the recorded data being used for the analysis. The pick-up in the APSP was reduced and a full study of four channels was made.

The pulse height distribution, for the sum of two strips, at the three nodes in the system for the non irradiated detector can be compared in figure 8. Shown in the same figure is the expected response from the APSP; it was calculated using the information in the ADB with the appropriate weights. The distributions are fitted with a Landau function describing the charge loss for minimum ionizing particles transversing the detector. The noise throughout the chain is presented in figure 9. The noise presented for the measured APSP noise is not common mode corrected. The correction is 54 mV r.m.s.

The performance in signal to noise in the system for the two detectors measured are shown in tables 1 and 2. In this test 20% of the charge was lost by the deconvolution. This is some more than expected but the level is acceptable considering the generous acceptance in timing and the perhaps not optimal pulse shape. The signal/noise ratio in the ADB compared with the preamplifier-shaper is within errors the same 22/1. An noise increase in the APSP was calculated to 30% which degraded the S/N in the APSP to about 13/1.

Table 1

The performance of the front-end connected to a non irradiated detector

Non irradiated	**Signal**	**Noise**	**S/N**
Amplifier-Shaper	53	2,4	22
ADB	59	2,7	22
APSP	463	38	12
APSP calculated	47	3,1	15

Table 2

The performance of the front-end connected to a electron irradiated detector

Electron irradiated	**Signal**	**Noise**	**S/N**
ADB	62	3,0	21
APSP	498	45	11

Finally the response from the APSP was studied by scanning the 45 ns RC-CR shaped signal. This study is important when trying to estimate the performance of a discriminator connected to the APSP. By moving the T1 in steps of 15 ns around the right time bin the response from the APSP was studied. In an ideal case the pulse height in bins outside the right one should be zero. On real data some contamination is expected because of the charge signal not being a clean delta pulse [6]. The APSP response was recorded at -15 ns, 15 ns and 30 ns delay compared with the right time bin. The data was analysed using the same cuts as described but shifting the data with the corresponding delay to the T1 trigger. The result obtained in this exercise is shown in figure 10. The source for the contamination of the signal in the neighbouring bins is mainly due to timing shifts and non optimal pulse shapes.

5. CONCLUSIONS

The functionality of a front-end design using a 45 ns preamplifier-shaper circuit, an analogue delay buffer and with a deconvolution filter has been tested in a 100 GeV pion beam. Except for some problems with gain mismatch and pick-up the functionality has been proven to work as designed. Detailed studies were performed in the laboratory. The conditions in the laboratory were comparable with the testbeam. The final response from the deconvolution in the APSP was both calculated and measured giving a signal to noise ratio before the deconvolution 22/1 and after the deconvolution 13/1 for two channel clusters to a single channel noise. A scan of the APSP was performed giving the contamination of the signal into the neighbouring time bin to less than 20%.

The results in this paper are obtained with the first prototypes of the front-end chain. The performance will improve when the full chain will be integrated to a full chip with each part matched to the other.

Acknowledgements

This work has been funded by CERN and KBN - The Polish State Committee for Scientific Research - (Poland). We should like to thank them both for their support.

References

[1] T. Høgh et al., *A Low Noise Low Power CMOS Charge Sensitive Amplifier for Silicon Detectors at LHC*, Presented at the Sixth European Symposium on Semiconductor Detectors, Milan, 1992.

[2] R. Brenner et al., *Design and Performance of an Analog Delay and Buffer Chip for Use with Silicon Strip Detectors at LHC*, CERN-PPE/93-.

[3] N. Bingefors et al., *A Novel Technique for Fast Pulse-Shaping Using a Slow Amplifier at LHC*, Nucl. Instr. and Meth. A326 (1992) 112.

[4] *RD20 P-Side Test Structures (IC/SI)*, RD20/TN3.

[5] H. Borner et al., *The Development of High Resolution Strip Detectors for Experiments at High Luminosity at the LHC*, CERN R&D Proposal CERN/DRDC 91-10.

[6] W. Dabrowski and M. Idzik, *Second-Order Effects in Front-End Electronics and APSP Robustness*, RD20/TN/15, March 1993.

Figure Captions

Fig. 1 : A schematic of the front-end electronic system proposed for LHC. The amplifier is followed by an analogue pipeline which delays the signal. At a positive 1st level trigger decision the data is serially transferred into an analogue processor to resolve the time information. Below the schematics a pulse is followed through the system. The cross-hatched bins are the samples used for the deconvolution. The single-hatched bin is the peak value used for the pulse height measurements.

Fig. 2 : The testbeam set-up with hodoscope and triggering logic.

Fig. 3 : The ADB and APSP clocking schematics.

Fig. 4 : A typical single event for two neighbouring channels seen after the Amplifier, ADB and APSP. The vertical scale is given in mV. The horizontal scale for the Amplifier and the ADB is 15 ns/bin and for the APSP 1 μs/bin.

Fig. 5 : Pulse heights for the difference of two neighbouring channels recorded from the output of the amplifier-shaper, ADB and APSP.

Fig. 6 : The calculated pulse height plotted versus the measured one in the APSP circuit.

Fig. 7 : Pulse-height distribution from the ADB in the testbeam (left) and the laboratory (right).

Fig. 8 : The pulse heights for the sum of two channels for the three nodes in the chain. The fourth distribution is the expected response for the APSP. The pulse height distributions are fitted with a landau function. The most probable peak given by P1 in the fit.

Fig. 9 : The noise distribution for the Amplifier-Shaper, the ADB and the APSP. The measured APSP noise has to be corrected for common mode.

Fig. 10 : The APSP response for the T1 trigger delayed by -15 ns, 0 ns , 15 ns and 30 ns.

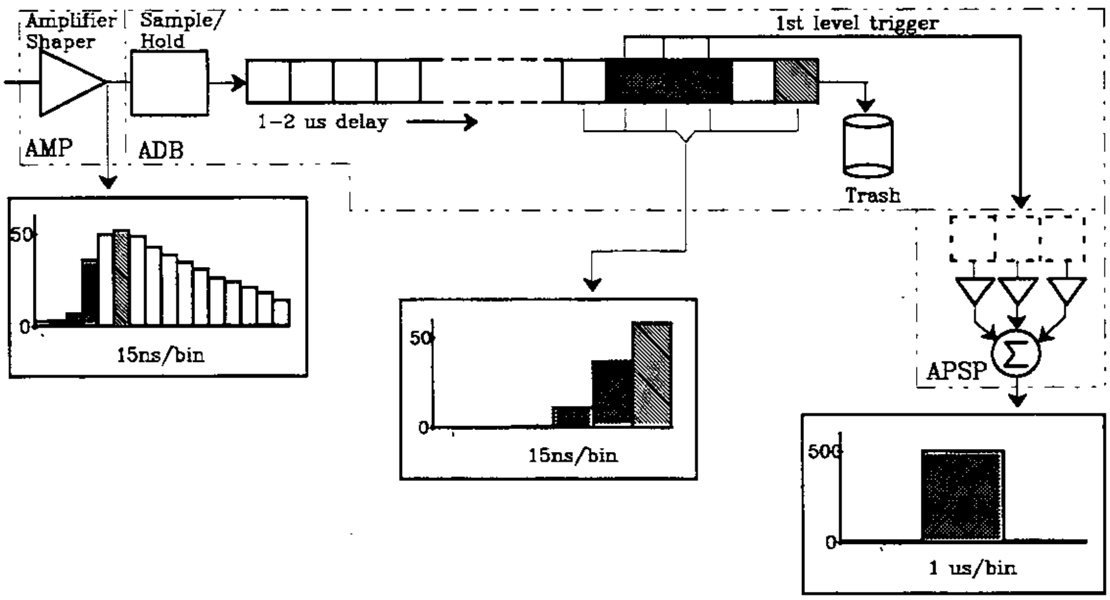
Amplifier
Shaper
Sample/
Hold
1st level trigger
1-2 us delay
AMP
ADB
Trash
50
0
15ns/bin
50
0
15ns/bin
APSP
500
0
1 us/bin

Figure 1

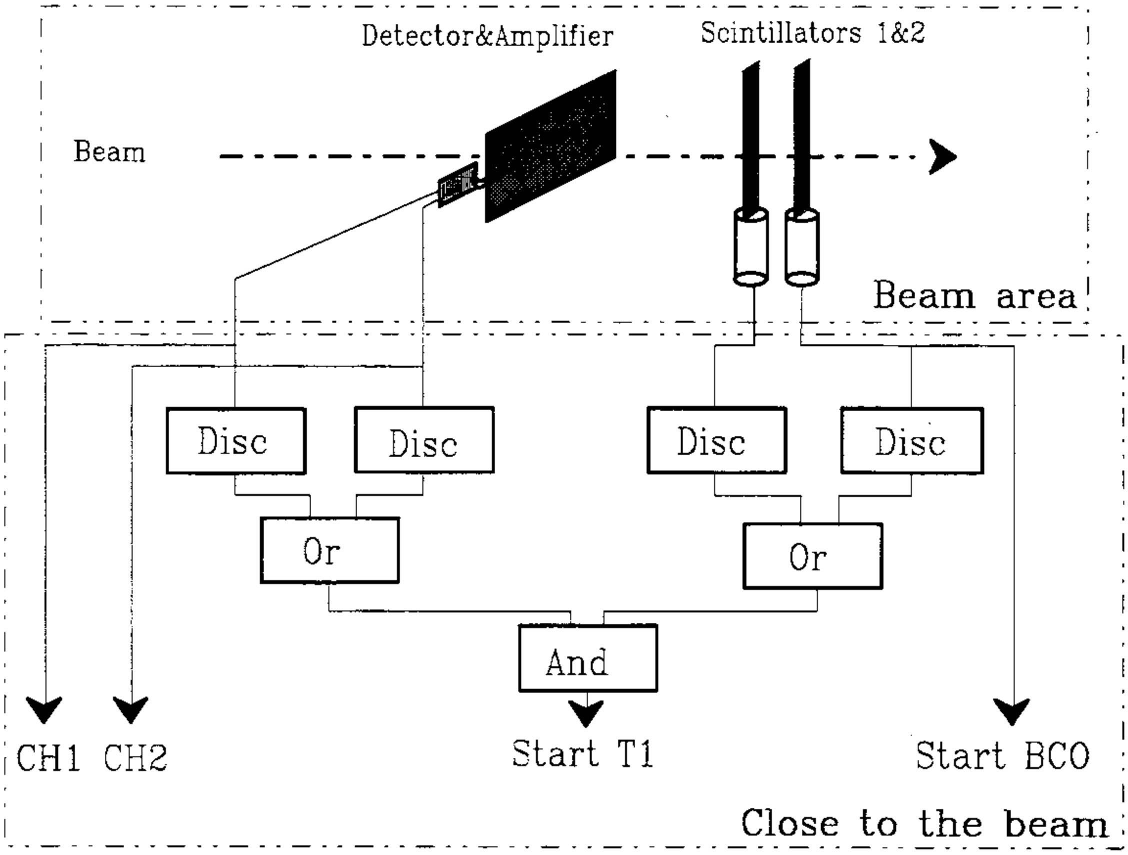
Detector&Amplifier
Scintillators 1&2
Beam
Beam area
Disc
Disc
Disc
Disc
Or
Or
And
CH1
CH2
Start T1
Start BCO
Close to the beam

Figure 2

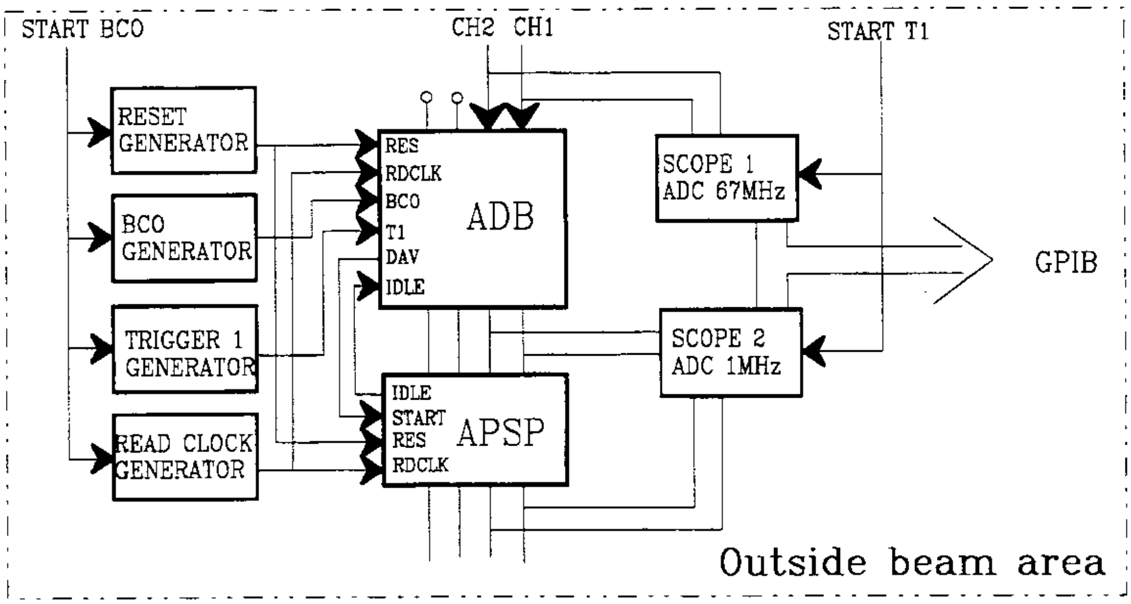
START BCO
CH2 CH1
START T1
RESET GENERATOR
BCO GENERATOR
TRIGGER 1 GENERATOR
READ CLOCK GENERATOR
RES
RDCLK
BCO
T1
DAV
IDLE
ADB
SCOPE 1 ADC 67MHz
SCOPE 2 ADC 1MHz
GPIB
IDLE
START
RES
RDCLK
APSP
Outside beam area

Figure 3

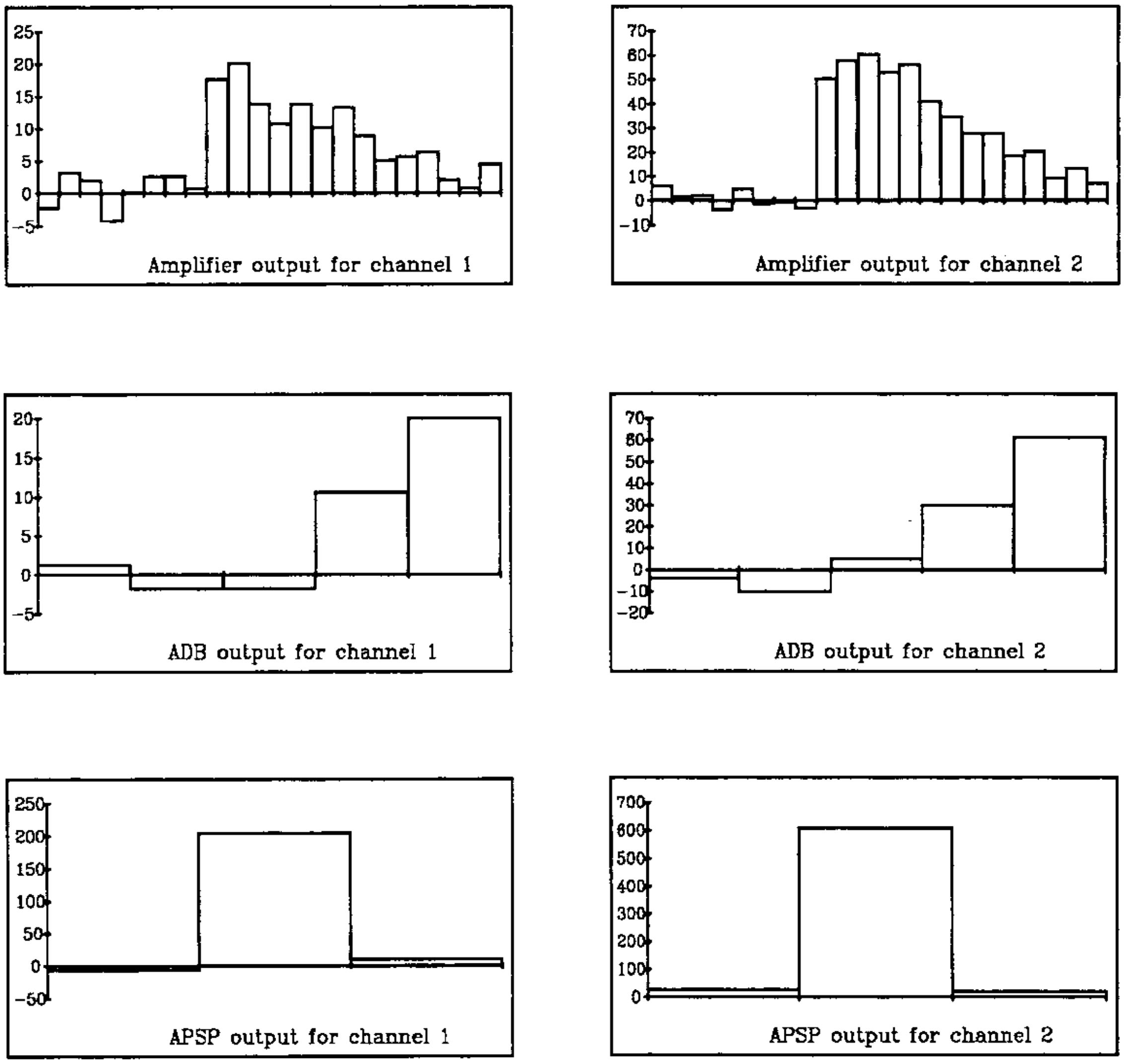
25
20
15
10
5
0
-5
Amplifier output for channel 1
70
60
50
40
30
20
10
0
-10
Amplifier output for channel 2
20
15
10
5
0
-5
ADB output for channel 1
70
60
50
40
30
20
10
0
-10
-20
ADB output for channel 2
250
200
150
100
50
0
-50
APSP output for channel 1
700
600
500
400
300
200
100
0
APSP output for channel 2

Figure 4

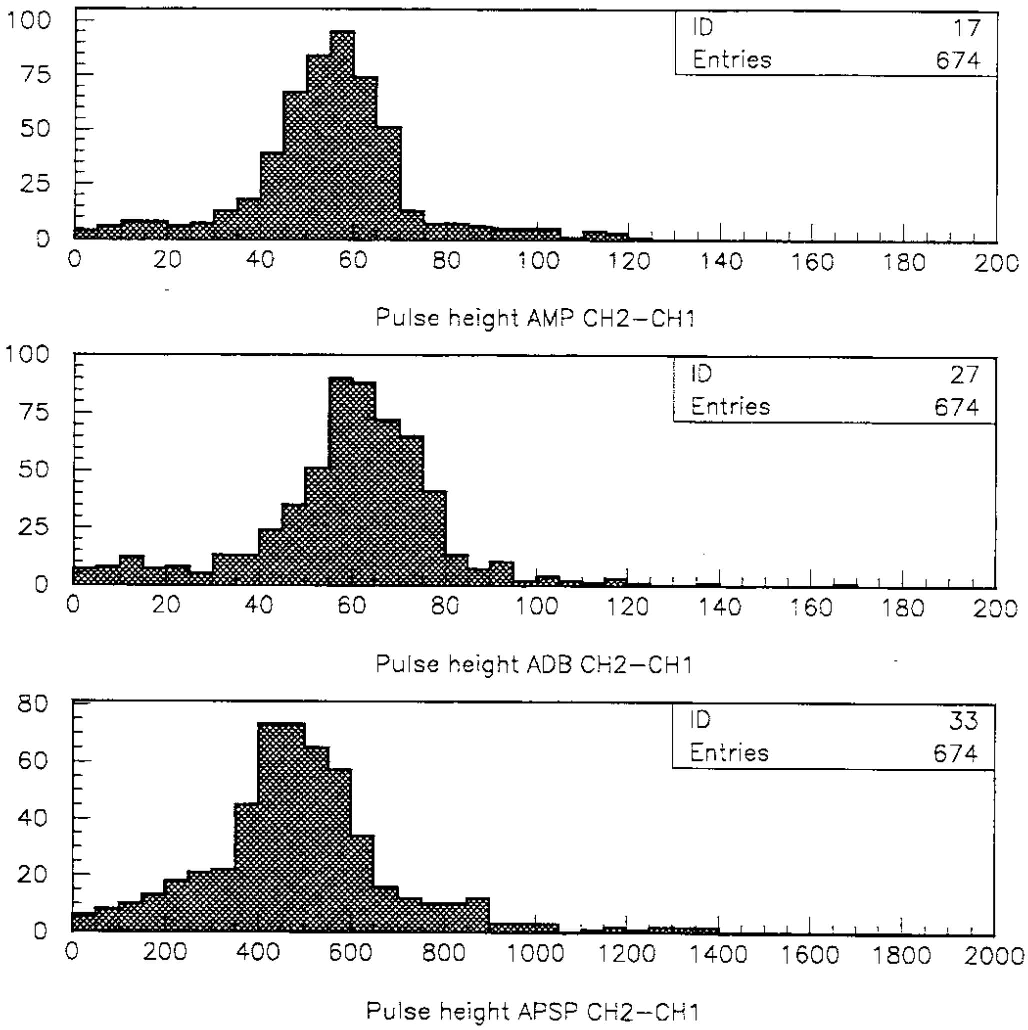

ID 17
Entries 674
Pulse height AMP CH2−CH1
ID 27
Entries 674
Pulse height ADB CH2−CH1
ID 33
Entries 674
Pulse height APSP CH2−CH1

Figure 5

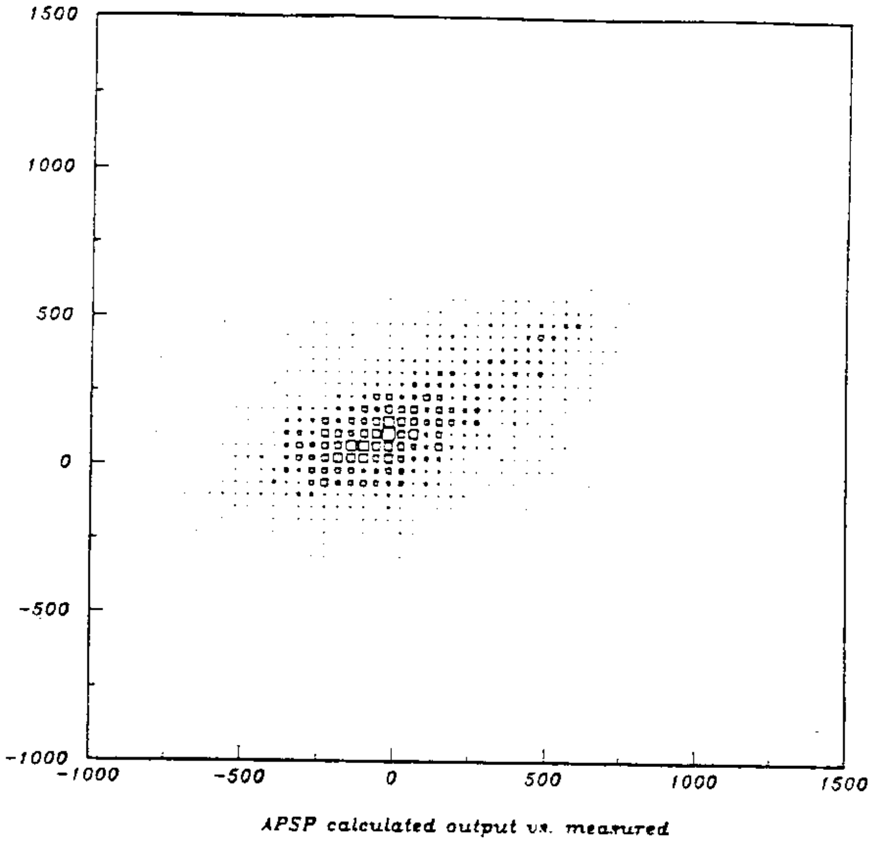
1500
1000
500
0
-500
-1000
-1000
-500
0
500
1000
1500
APSP calculated output vs. measured

Figure 6

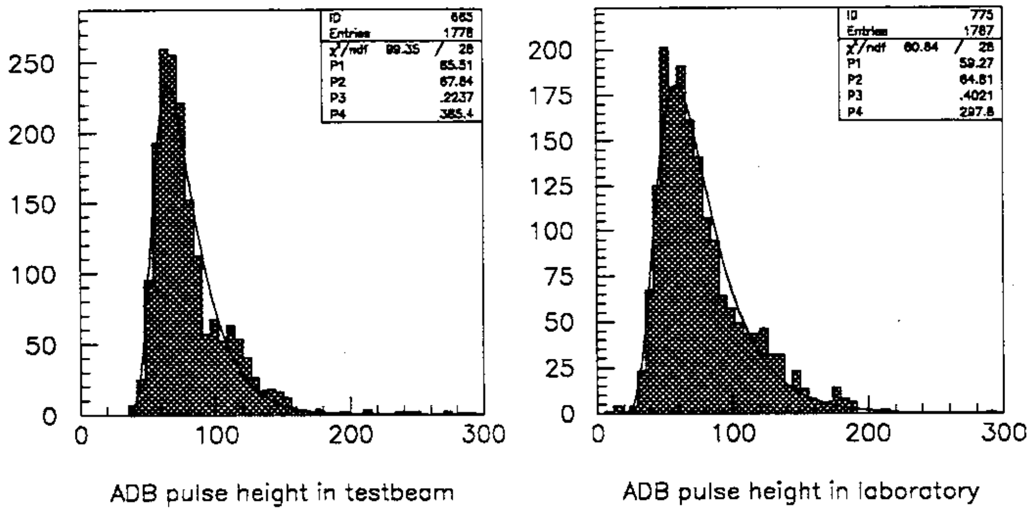
ID 663
Entries 1778
χ²/ndf 99.35 / 28
P1 65.51
P2 67.84
P3 .2237
P4 385.4
0
50
100
150
200
250
0
100
200
300
ADB pulse height in testbeam
ID 775
Entries 1787
χ²/ndf 60.84 / 28
P1 59.27
P2 64.81
P3 .4021
P4 297.8
0
25
50
75
100
125
150
175
200
0
100
200
300
ADB pulse height in laboratory

Figure 7

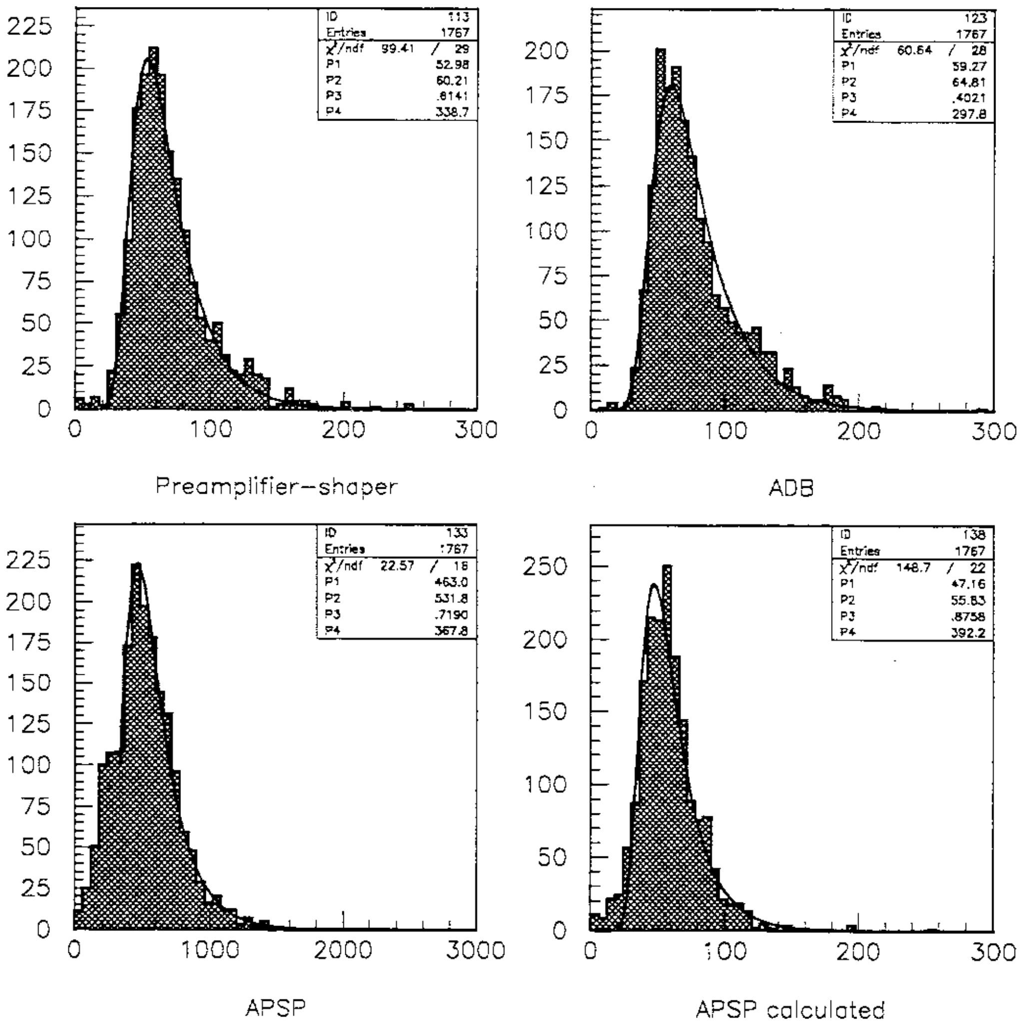
ID 113
Entries 1767
χ²/ndf 99.41 / 29
P1 52.98
P2 60.21
P3 .6141
P4 338.7
Preamplifier−shaper
ID 123
Entries 1767
χ²/ndf 60.64 / 28
P1 59.27
P2 64.81
P3 .4021
P4 297.8
ADB
ID 133
Entries 1767
χ²/ndf 22.57 / 18
P1 463.0
P2 531.8
P3 .7190
P4 367.8
APSP
ID 138
Entries 1767
χ²/ndf 148.7 / 22
P1 47.16
P2 55.83
P3 .8758
P4 392.2
APSP calculated

Figure 8

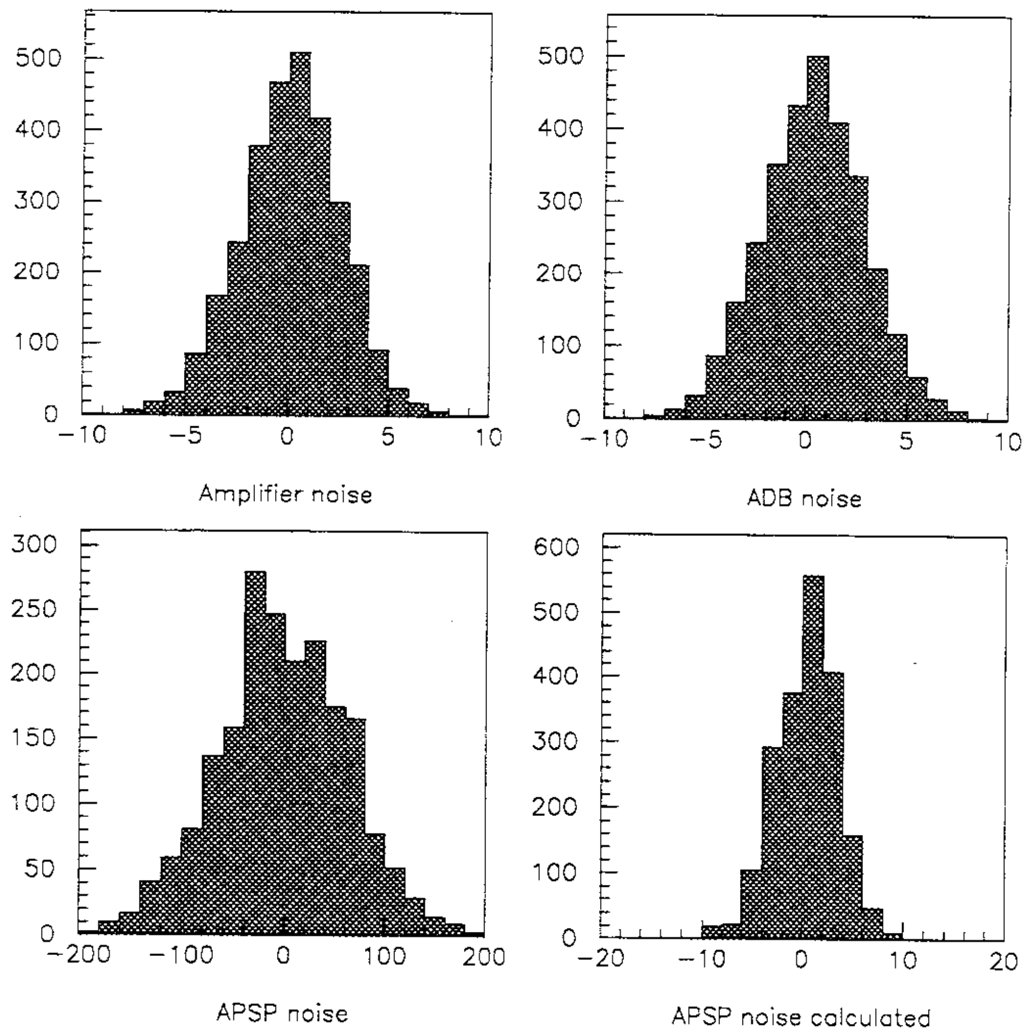

500
400
300
200
100
0
−10
−5
0
5
10
Amplifier noise
ADB noise
300
250
200
150
100
50
−200
−100
100
200
APSP noise
600
−20
20
APSP noise calculated

Figure 9

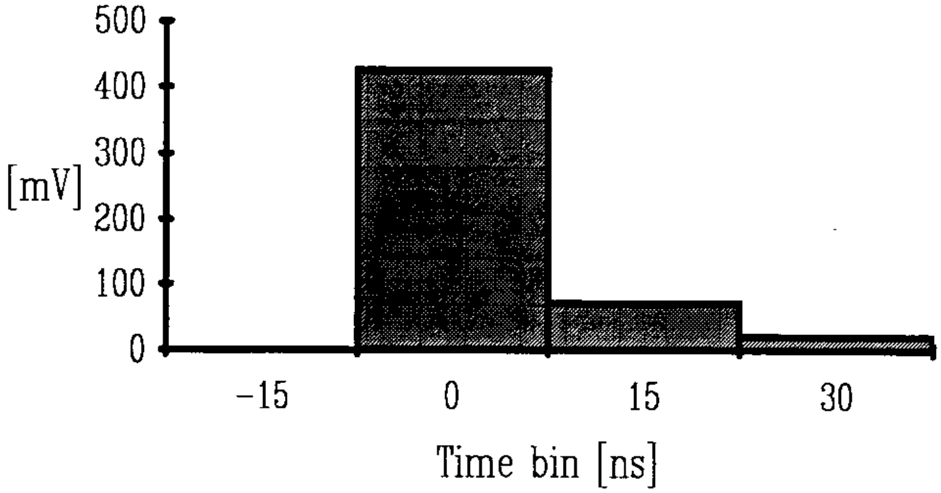

Figure 10